Nucleon gravitational form factors and radii in holographic QCD

Kiminad Mamo
University of Connecticut

NREC 2026 CFNS Workshop
Stony Brook University

April 17, 2026

References

This talk is based on:

- **1910.04707** (PRD) — diffractive J/ψ (with Ismail Zahed).
- **2204.08857** (PRD) — D-term inclusion (with Ismail Zahed).
- **2106.00752** (NPB) — electromagnetic form factors (with Ismail Zahed).
- **2604.12037** — DDVCS/DVCS.

AdS/CFT

- The AdS/CFT correspondence can be used to compute correlation functions of local operators [Maldacena:1998; Gubser, Klebanov, Polyakov:1998; Witten:1998]

$$Z_{\text{gauge}}(J\mathcal{O}, N_c, \lambda) \equiv Z_{\text{gravity}}(\phi_0, g_5, \alpha'/R^2), \quad \text{where } J \equiv \phi_0.$$

- Correlation functions are evaluated via Witten diagrams in AdS.
- For non-conformal theories with a mass gap (dual to a deformed AdS background), scattering amplitudes can likewise be computed using these Witten diagrams in AdS

$$ds^2 = \frac{R^2}{z^2}(\eta_{\mu\nu}\, dx^\mu dx^\nu - dz^2), \quad \eta_{\mu\nu} = \mathrm{diag}(1, -1, -1, -1),$$

with $0 \leq z \leq \infty$, connects the UV boundary ($z \to 0$) to the IR ($z \to \infty$), and mass gap/confinement induced by a background dilaton field $\phi(z) = \kappa^2 z^2$.

From vacuum to hadron: why holographic QCD is anchored

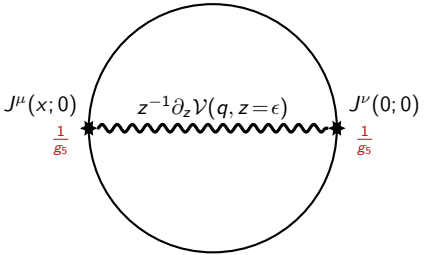

Vacuum current correlator

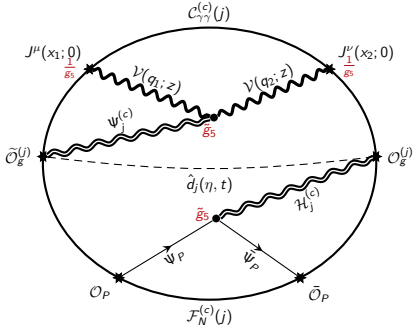

Hadronic current–current correlator after fixed-j factorization

$$\Pi_V(Q^2) \sim -\frac{N_c}{24\pi^2} \ln Q^2 \implies g_5^2 = \frac{12\pi^2}{N_c}.$$

[Erlich–Katz–Son–Stephanov:2005]

UV matched to pQCD; IR encoded in conformal moments and wavefunction overlaps. [KM:2026]

Soft-wall spectral representation

Soft-wall bulk-to-boundary propagator [Grigoryan–Radyushkin:2007]

$$\mathcal{V}(Q,z) = g_5 \sum_{n=0}^{\infty} \frac{F_n\,\phi_n(z)}{Q^2+m_n^2} = \Gamma\!\left(1+\frac{Q^2}{4\kappa^2}\right)\kappa^2 z^2\,\mathcal{U}\!\left(1+\frac{Q^2}{4\kappa^2};2;\kappa^2 z^2\right).$$

- The pole sum is the spectral representation behind **two-point**, **three-point**, and **four-point** correlators.
- For off-forward hadronic current correlators the UV kernel is universal; all hadron structure sits in conformal moments. [Nishio-Watari:2014,KM:2026]

$$\mathcal{H}^{(X)}_{\rm holo}(j) \sim \xi^{-j}\,{}_2F_1\!\left(\ldots;\frac{\eta^2}{\xi^2}\right)\,\Phi_N^{(X)}(j,t,\eta).$$

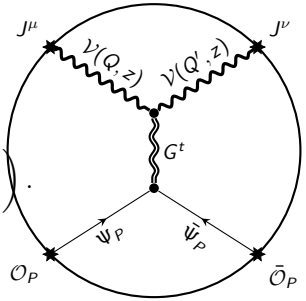

Same $\mathcal{V}(Q,z)$ enters the 2-point and 3-point sectors.

Spin-1 (Electromagnetic) form factors: Witten-diagram picture

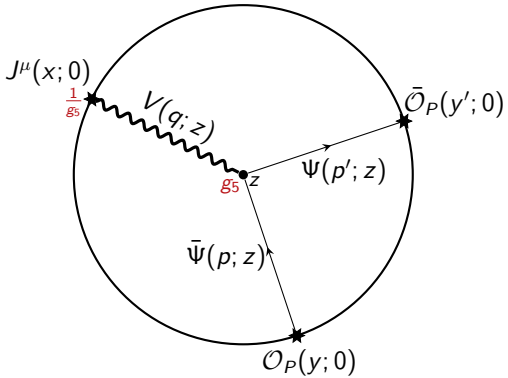

Vector-meson tower exchange in the bulk

Current matrix element

$$\langle p'|J^\mu_{\rm em}(0)|p\rangle = \bar{u}(p')\Big[F_1(Q^2)\gamma^\mu + F_2(Q^2)\frac{i\sigma^{\mu\nu}q_\nu}{2m_N}\Big]u(p).$$

- The Sachs combinations are

$$G_E = F_1 - \frac{Q^2}{4m_N^2}F_2, \qquad G_M = F_1 + F_2.$$

- In soft-wall holographic QCD the same spectral propagator $\mathcal{V}(Q,z)$ enters the three-point function, so the low-Q^2 slopes are controlled by the same κ and twist input that controlled the two-point function.[Abidin–Carlson:2009]

Soft-wall predictive strategy

Two practically equivalent EM calibrations

Choice	Fixing	Values
fit-driven	large-Q power counting + G_M^p	$\tau = 3$, $\kappa = 0.402$ GeV
spectroscopy-driven	m_N, m_ρ	$\tau = 2.465$, $\kappa = 0.388$ GeV

Same $\mathcal{V}(Q, z)$ enters the 2-point and 3-point sectors.

Practical message

Fix τ, κ once: low-Q^2 slopes and many radii then become predictions.

Spin-1 (Electromagnetic) Form Factors of Proton

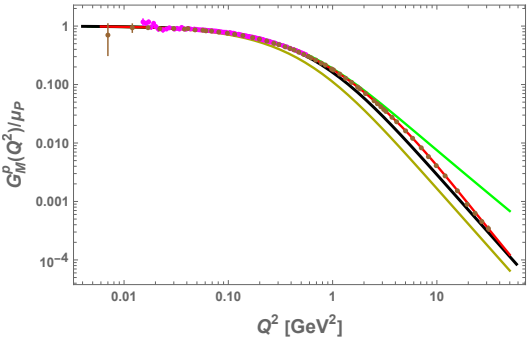

(a)

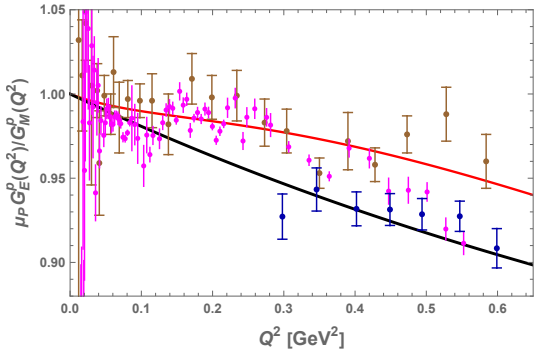

(b)

Figure: Black curves: soft-wall holographic QCD with $\tau = 3$, $\kappa = 0.402$ GeV fixed from the proton magnetic form factor. Green curves: spectroscopy-driven choice $\tau = 2.465$, $\kappa = 0.388$ GeV. Brown, magenta, and dark-blue points denote world, Mainz A1, and JLab recoil-polarization data, respectively.

Spin-1 (Electromagnetic) Form Factors of Proton

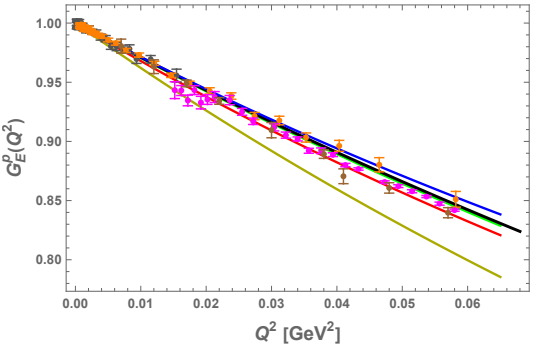

(a)

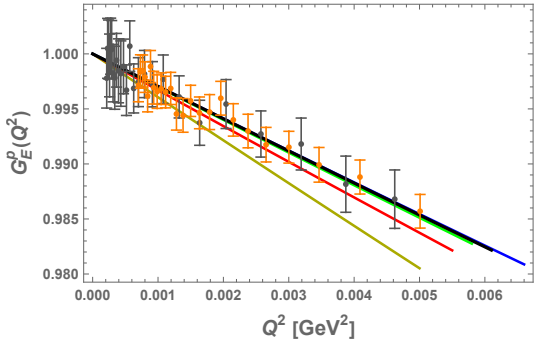

(b)

Figure: Brown data points (with Arrington-2007 red-fit) are the world data, Magenta data points are the Mainz A1 data [Bernauer:2013], and orange and gray data points (with its PRad blue-fit) are the PRad data [Xiong:2019].

Spin-1 (Electromagnetic) Form Factors of Proton

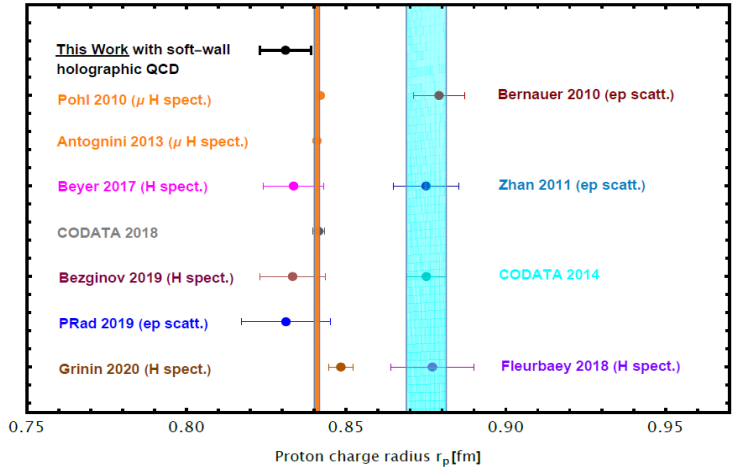

Figure: Charge radius of the proton.

Electromagnetic radii: proton comparison plot

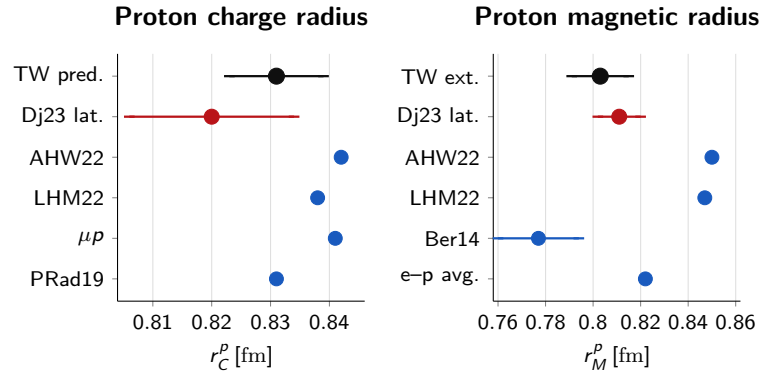

Black = soft-wall holographic QCD (**pred.**/**ext.**) **Red** = lattice QCD [Djukanovic et al.:2023]
Blue = experiment / data-driven theory analyses

Electromagnetic radii: neutron comparison plot

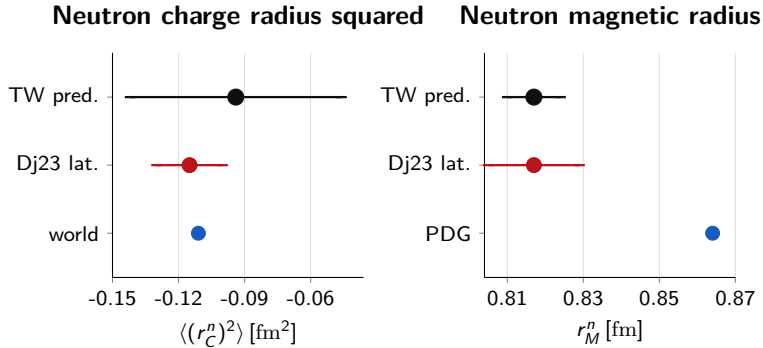

Once τ and κ are fixed, the neutron magnetic radius and the negative neutron charge radius-squared emerge as nontrivial predictions compatible with modern lattice and world averages.

Nucleon gravitational form factors: what is being extracted?

Energy–momentum tensor decomposition

$$\langle p'|\, T_a^{\mu\nu}(0)|p\rangle = \bar{u}(p')\left[A_a(t)\,\gamma^{(\mu}P^{\nu)} + B_a(t)\,\frac{P^{(\mu}\mathrm{i}\sigma^{\nu)\rho}\Delta_\rho}{2m_N} + D_a(t)\,\frac{\Delta^\mu\Delta^\nu - g^{\mu\nu}\Delta^2}{4m_N}\right]u(p) + \cdots$$

with $P = (p' + p)/2$, $\Delta = p' - p$, $t = \Delta^2$, and $D_a(t) = 4\,C_a(t)$.

- $A_a(t)$: momentum / mass form factor.
- $B_a(t)$: gravitomagnetic form factor; together with A_a it controls angular momentum. [Ji:1996]
- $D_a(t)$: mechanical form factor; it governs pressure and shear distributions. [Polyakov-Schweitzer:2003-2018]
- For near-threshold heavy-quarkonium production the two protagonists are the gluonic $A_g(t)$ and $D_g(t)$.

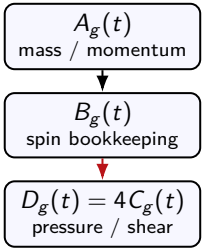

Witten-diagram intuition in soft-wall holographic QCD

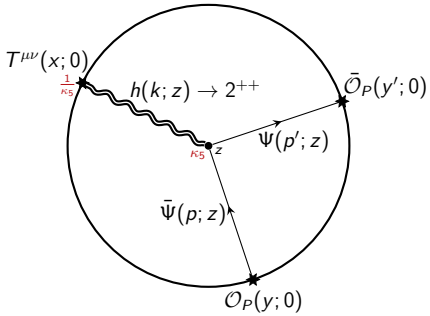

Spin-2 / tensor channel

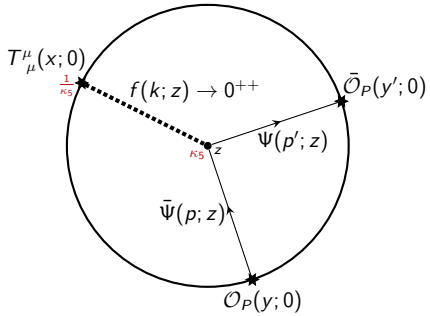

Spin-0 / scalar completion

$A_g(t) \iff 2^{++}$ glueball/tensor exchange

$D_g(t)$ is fixed by the tensor–scalar difference

Key physical point

The scalar 0^{++} channel is essential for the D-term; tensor exchange alone only fixes $A_g(t)$.

Soft-wall outputs: $A_g(t)$ and $D_g(t)$ versus lattice

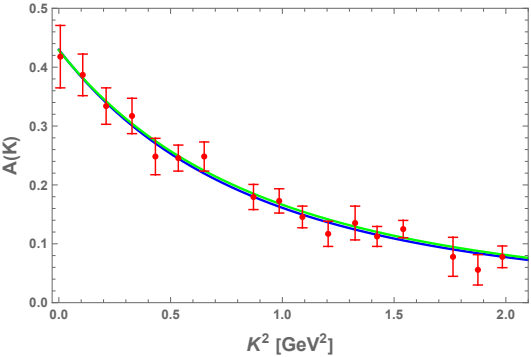

(a) $A_g(t)$

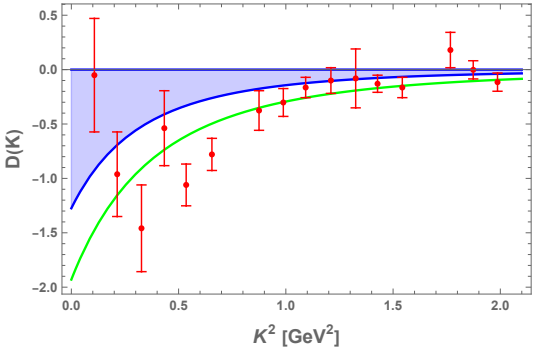

(b) $D_g(t) = 4C_g(t)$

Figure: Representative lattice comparison: red points denote lattice data [Pefkou-Hackett-Shanahan:2021] and the black/blue soft-wall curve is the holographic output. The same framework that organizes low-Q^2 electromagnetic slopes also gives sensible gluonic EMT form factors.

Why near-threshold J/ψ is a particularly clean experimental lever arm

- Heavy quarkonium behaves as a compact color dipole: this strongly filters **gluonic** dynamics. [Kharzeev:1996]
- Near threshold, the amplitude is especially sensitive to the **lowest gluonic moments**, i.e. to the EMT form factors rather than to a large tower of unrelated soft mechanisms [Hatta-Yang:2018, KM-Zahed:2019, Guo-Ji-Liu:2021, Kharzeev:2021].
- So this process is experimentally attractive because it is not just "another exclusive channel"; it is a clean lever arm on $A_g(t)$ and $D_g(t)$.

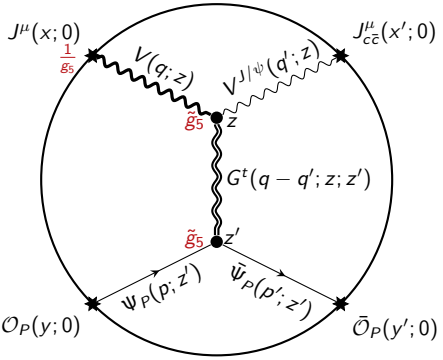

From the amplitude to the extraction of $A_g(t)$ and $D_g(t)$

Near-threshold structure of the differential cross section

$$\frac{\mathrm{d}\sigma}{\mathrm{d}t} = \mathcal{N}^2 \left[A_g(t) + \xi^2 D_g(t)\right]^2 \frac{1}{A_g^2(0)} \frac{1}{128\pi(s-m_N^2)^2} F(s,t,M_{J/\psi},m_N) \left(1 - \frac{t}{4m_N^2}\right).$$

- $A_g(t)$ is the leading tensor contribution.
- $D_g(t)$ enters with an additional kinematic lever arm but is essential for the scalar/mechanical channel.
- In other words, the experimentally extracted t-dependence is not just a radius fit; it carries direct information on the stress tensor decomposition.

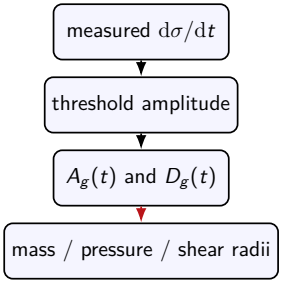

What I want experimentalists to take away

Near-threshold J/ψ is a way of fitting **specific gluonic matrix elements**, not just an effective slope parameter.

J/ψ-007 extraction: gluonic $A_g(t)$ and $D_g(t)$

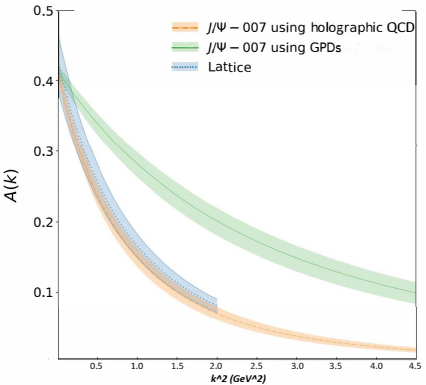

(a) $A_g(t)$

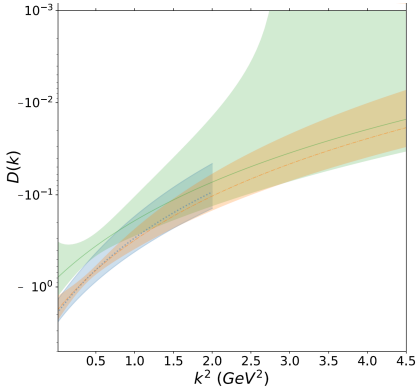

(b) $D_g(t) = 4C_g(t)$

Figure: J/ψ-007 near-threshold extraction and comparison to data. This is the first dedicated experimental handle on the same gluonic $A_g(t)$ and $D_g(t) = 4C_g(t)$ language used on the theory side.

Recent CLAS12 extraction: gluonic $A_g(t)$ and $C_g(t)$

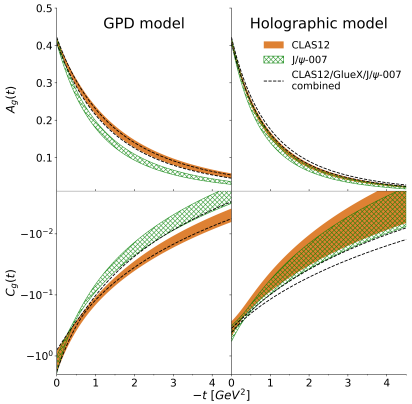

Figure: Actual CLAS12 comparison figure showing the extraction of gluonic $A_g(t)$ and $C_g(t)$ in GPD-based [Guo et al.:2021] and holographic analyses.

From $D_g(t)$ to pressure and shear

Breit-frame mechanical imaging

$$p(r),\ s(r) \ \propto \ \int \frac{\mathrm{d}^3\boldsymbol{\Delta}}{(2\pi)^3}\, \mathrm{e}^{\,\mathrm{i}\boldsymbol{\Delta}\cdot\boldsymbol{r}}\, D_g(t), \qquad t=-\boldsymbol{\Delta}^2.$$

- $D_g(t)$ controls the mechanical stress tensor: pressure in the core, an attractive outer region, and the shear-force profile.
- Together with $A_g(t)$, it sets the mass, scalar, and mechanical radii extracted from the same gluonic form-factor framework.
- This gives a direct visual bridge between soft-wall holography, lattice QCD, and near-threshold J/ψ data.

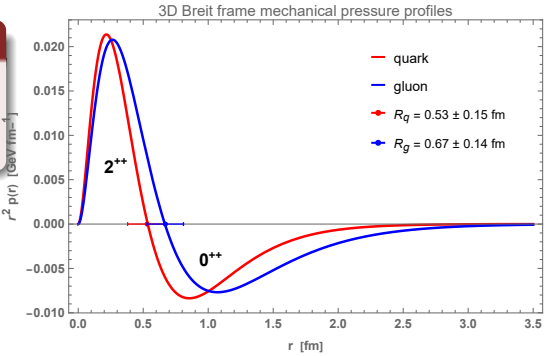

Scalar and Mass Radii of Proton

Definitions from the gluonic energy–momentum tensor

The same soft-wall $A(K)$ and $D(K)$ form factors shown earlier also define the proton's gluonic scalar and mass radii [Ji:2021].

Scalar radius r_{GS}

Derived from the trace T^{μ}_{μ}:

$$\langle r^2_{GS}\rangle = -\frac{6}{A_S(0)}\left.\frac{dA_S(K)}{dK^2}\right|_0$$

with

$$A_S(K) \equiv A(K) + \frac{3K^2}{4m_N^2}D(K)\,.$$

Mass radius r_{GM}

Derived from the 00 component of the EMT:

$$\langle r^2_{GM}\rangle = -\frac{6}{A_M(0)}\left.\frac{dA_M(K)}{dK^2}\right|_0$$

with

$$A_M(K) \equiv A(K) + \frac{K^2}{4m_N^2}D(K)\,.$$

These are the radii extracted from the same holographic A and D inputs used in the gluonic GFF analysis. For $D(K) = 0$, we have $\langle r^2_{GM}\rangle = \langle r^2_{GS}\rangle$ [Kharzeev:2021]

Scalar and Mass Radii of Proton

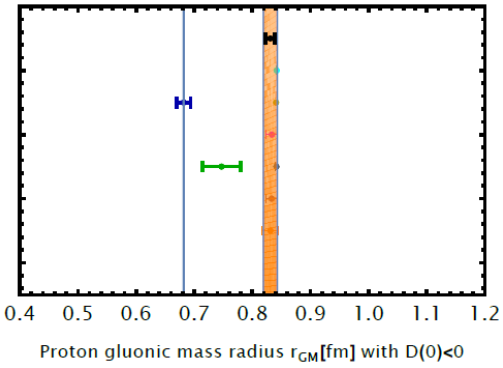

(a) Proton gluonic mass radius r_{GM}

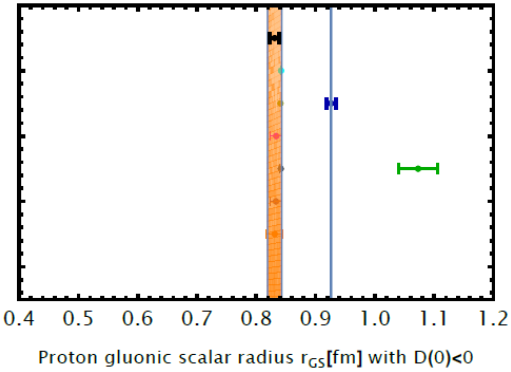

(b) Proton gluonic scalar radius r_{GS}

Figure: Blue point: result obtained from our holographic A and D form factors, $(r_{GM}, r_{GS}) = (0.682 \pm 0.012\ \text{fm},\ 0.926 \pm 0.008\ \text{fm})$. Green point: result obtained from the lattice tripole fit to the lattice A and D form factors, $(r_{GM}, r_{GS}) = (0.747 \pm 0.033\ \text{fm},\ 0.926 \pm 0.008\ \text{fm})$ [Pefkou-Hackett-Shanahan:2021].

Why this is useful for NREC: low-Q^2 radii, lattice, and JLab

- **On the EM side:** once τ and κ are fixed, the soft-wall extrapolation to very small Q^2 is sharply constrained.
- **On the gravitational side:** the same framework links lattice GFFs and near-threshold J/ψ data.
- **Experimentally:** PRad II can directly test the extreme low-Q^2 extrapolation of the soft-wall black curve, while CLAS12 and future quarkonium measurements test the gluonic EMT sector.
- **Conceptually:** the electromagnetic-radius community and the gravitational-form-factor community are really studying different projections of the same broad correlator technology.

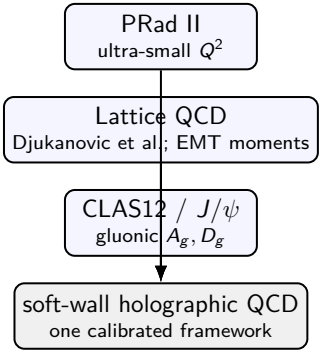

Summary

- The holographic construction is **anchored**, not ad hoc: the UV current correlator is matched to pQCD, and the same Witten-diagram technology generates spectral representations for two-, three-, and four-point functions.
- In the electromagnetic sector, once τ and κ are fixed by power counting plus G_M^p — or equivalently by m_N and m_ρ — the proton charge radius and the neutron radii are largely predictions and compare well with modern data and lattice QCD.
- In the gravitational sector, the tensor 2^{++} and scalar 0^{++} channels naturally generate $A_g(t)$ and $D_g(t)$, and the soft-wall outputs are compatible with the broad lattice picture.
- Near-threshold J/ψ photoproduction is therefore a particularly clean experimental handle on **gluonic stress correlations** in the nucleon.
- For this NREC audience, the practical punchline is simple: **PRad II can test the low-Q^2 soft-wall extrapolation, while CLAS12 tests the gluonic EMT side of the same framework.**

Thank you

Backup: closed-form soft-wall electromagnetic form factors

Dirac and Pauli form factors

$$\langle p'|J^{\mu}_{\rm em}(0)|p\rangle = \bar{u}(p')\left(F_1(Q^2)\gamma^{\mu} + F_2(Q^2)\frac{i\sigma^{\mu\nu}q_{\nu}}{2m_N}\right)u(p).$$

$$F_1^P(Q,\kappa,\tau) = \left(\frac{a}{2}+\tau\right)B(\tau,a+1) + \eta_P[\tau]\,(\tau-1)\,\frac{a(a(\tau-1)-1)}{(a+\tau)(a+\tau+1)}\,B(\tau-1,a+1),$$

$$F_2^P(Q,\kappa,\tau) = \eta_P[\tau]\,4(\tau-1)\,\tau\,B(\tau,a+1),$$

$$F_1^N(Q,\kappa,\tau) = \eta_N[\tau]\,(\tau-1)\,\frac{a(a(\tau-1)-1)}{(a+\tau+1)(a+\tau)}\,B(\tau-1,a+1),$$

$$F_2^N(Q,\kappa,\tau) = \eta_N[\tau]\,4(\tau-1)\,\tau\,B(\tau,a+1),$$

with

$$a = \frac{Q^2}{4\kappa^2}, \qquad \eta_P[\tau] = \frac{1.793}{4(\tau-1)}, \qquad \eta_N[\tau] = \frac{-1.913}{4(\tau-1)}.$$

$$G_E^{p,n} = F_1^{p,n} - \frac{Q^2}{4m_N^2}F_2^{p,n}, \qquad G_M^{p,n} = F_1^{p,n} + F_2^{p,n}.$$

Backup: parameter choices and the predictive logic

Model	κ	τ	m_ρ^2 (GeV^2)	m_N^2 (GeV^2)	r_C^p (fm)
This work (spectroscopy-driven)	0.388	2.465	0.775^2 (exp.)	0.938^2 (exp.)	0.839 (pred.)
This work (fit-driven)	0.402	3.000	0.804^2 (pred.)	1.137^2 (pred.)	**0.831** (pred.)
Abidin–Carlson 2009	0.350	3.000	0.700^2 (pred.)	0.990^2 (pred.)	0.961 (pred.)

Predictive logic

- Fix τ from large-Q power counting and κ from G_M^p, or fix (τ, κ) from (m_N, m_ρ).
- After that, the remaining low-Q^2 proton and neutron radii are not independently tuned.